Neutron diffraction and specific heat studies on the magnetic ordering in the $[Fe^{II}(\Delta)Fe^{II}(\Lambda)(ox)_2(Phen)_2]_n$ molecular magnet

C. J. Ho,[1] J. L. Her,[1] C. P. Sun,[1] C. C. Yang,[2] C. L. Huang,[1] C. C. Chou,[1] Lu-Lin Li,[3] K. J. Lin,[3] W. H. Li,[2] J. W. Lynn,[4] and H. D. Yang[1,*]

[1]*Department of Physics, Center of Nanoscience and Nanotechnology, National Sun Yat-Sen University, Kaohsiung 804, Taiwan*

[2]*Department of Physics and Center for Neutron Beam Applications, National Central University, Chung-Li 32054, Taiwan*

[3]*Department of Chemistry, Center of Nanoscience and Nanotechnology, National Chung-Hsing University, Taichung 402, Taiwan*

[4]*NIST Center for Neutron Research, National Institute of Standards and Technology, Gaithersburg, Maryland 20899, USA*

(Received 31 March 2007; revised manuscript received 5 October 2007; published 19 December 2007)

The magnetic characteristics of the molecular magnet $[Fe^{II}(\Delta)Fe^{II}(\Lambda)(ox)_2(Phen)_2]_n$, having chemical formula $C_{28}H_{16}Fe_2N_4O_8$ for unity, has been studied by magnetization, neutron diffraction, and field-dependent specific heat-measurements. In the high-temperature regime ($T > T_m$), the one-dimensional Ising chain model with alternate Landé factors is applied to describe its quasiferrimagnetic behavior as temperature approaches T_m. In the low-temperature region ($T < T_m$), the increase of interchain interactions gives rise to long-range magnetic ordering as indicated by an anomaly in specific heat. Furthermore, an intrinsic antiparallel alignment of spins with a net ferrimagnetic structure is deduced from neutron diffraction study. The field-dependent λ-type anomaly of specific heat indicates that applying a magnetic field raises magnetic ordering temperature. An additional small anomaly in specific heat is also seen below T_m, which could be due to the zero-field splitting caused by the internal crystal field.

DOI: 10.1103/PhysRevB.76.224417 PACS number(s): 75.50.Xx, 61.12.Ld, 65.40.−b

I. INTRODUCTION

The field of molecular magnets is an emerging area and has received intensive study due to its potential applications in magnetic devices, such as magnetic memory.[1] The magnetic behavior of the molecules that changes with dimension is an attractive academic topic as the state of the system whether bulk or nanoscale particles is greatly controlled by its dimensionality. While the bulk shows spontaneous magnetization below critical temperature T_c, the nanoscale particles have nearly independent magnetic interactions. Researchers have tried to realize these magnetic properties by investigating the relationships among chelate molecules, magnetic centers, and connecting bridges between magnetic centers. Each of them plays an important role in constructing magnetic interactions. Due to the interest in these topics, the categories of research in the molecular magnets are usually complex and are continually renewed by researchers' efforts.[2–9]

One of the well-known molecular magnets is $Mn_{12}Ac$, which was first synthesized in 1980.[10] Its ground state composed of spin number $S=10$ was confirmed by high magnetic field and ac susceptometry experiments.[11–13] Through comprehensive studies, $Mn_{12}Ac$ is considered to be a well-described candidate for a single-molecule magnet (SMM), which reveals slow relaxation in magnetization and quantum tunneling phenomena at very low temperatures.[14] Another type of molecular magnet called single-chain molecular magnet (SCM), by analogy to SMM, has been investigated since 2001.[15] SCM type molecular magnets are composed of individual chains in which their intrachain interactions are 10^4 larger than interchain interactions, making them behave as magnets.[16] Though long-range ordering in pure one-dimensional (1D) materials only occurs at $T=0$ K, strong intrachain and/or interchain interactions form a two-dimensional (2D) or three-dimensional (3D) network, rendering the long-range magnetic ordering (LRMO) possible at finite temperatures. However, the limitations of producing SCM for industrial applications seem less than that of SMM. This is the reason why study on SCM has quickly become more active.[17]

In this work, we focus on the newly synthesized compound $[Fe^{II}(\Delta)Fe^{II}(\Lambda)(ox)_2(Phen)_2]_n$,[18] which includes two locally distinct Fe^{II} ions as the magnetic centers. Every Fe^{II} connects with two nitrogen atoms of the phen group while linking with each other with an oxalate that serves as a bridge of four oxygen atoms, thus forming a zigzag chain. The π-π interactions within the phen groups between the zigzag chains develop a quasi-2D framework within the *ac* plane, and hence, the magnetic properties of $[Fe^{II}(\Delta)Fe^{II}(\Lambda)(ox)_2(Phen)_2]_n$ may be strongly correlated with the dimensionality. In our previous paper,[18] the magnetic hysteresis was observed below 8.6 K, and was associated with the ferromagnetic (or ferrimagnetic) interactions. However, the negative Curie-Weiss temperature was derived from the magnetic susceptibility measurement, indicating the negative exchange interaction among magnetic Fe^{II} ions. It follows that the ground state of $[Fe^{II}(\Delta)Fe^{II}(\Lambda)(ox)_2(Phen)_2]_n$ could be canted-antiferromagnetic or ferrimagnetic. In order to solve this problem, in this paper, we have applied an Ising-like model, assigning Landé factors of Fe^{II} ions of different environments with different magnitudes. Due to this improvement, we have been able to reproduce the magnetic susceptibility correctly and also achieve the short-range ferrimagnetism present in the system.[19] To further explore the nature of the magnetic ordering of $[Fe^{II}(\Delta)Fe^{II}(\Lambda)(ox)_2(Phen)_2]_n$, including the configuration of spins and the dimension of ordering, the neutron diffraction and magnetic-field-dependent specific heat measurements have also been performed.

II. EXPERIMENTAL METHODS

Dark reddish single crystal $[Fe^{II}(\Delta)Fe^{II}(\Lambda)(ox)_2(Phen)_2]_n$ (the chemical formula for unity is $C_{28}H_{16}Fe_2N_4O_8$) is prepared by hydrothermal synthesis. It gives a highly reproducible yield of 62% by heating the reaction mixture of $FeCl_2 \cdot 4H_2O$, oxalic acid, phen, and water in molar ratios of 2:3:2:4400 at 180 °C for 96 h.[18] The superconducting quantum interference device magnetometer (MPMS XL-7) of Quantum Design has been used to measure the magnetic susceptibility under zero-field cooling (ZFC) and field cooling processes within the temperature range 2–300 K. Neutron diffraction experiments were performed at the NIST Center for Neutron Research (NCNR). The high-resolution neutron powder diffraction patterns were collected on the BT-1 powder diffractometer, with an incident wavelength of 1.541 Å, employing a Cu (311) monochromator crystal, and 15′-20′-7′ full width at half maximum angular collimations. The high-intensity neutron powder diffraction patterns were taken on the BT-9 triple-axis spectrometer, employing a pyrolytic graphite PG (002) monochromator crystal to select an incident wavelength of 2.359 Å. The magnetic intensity has been increased by coarse collimations, and a PG filter has been used to suppress a higher-order wavelength contamination if present in the beam and then a PG (002) analyzer crystal has been used to discriminate against inelastic scattering. A pumped ^{4}He cryostat was used to control the sample temperature for neutron diffraction measurements. A heat-pulse thermal relaxation calorimeter with ^{3}He cryostat was used to measure the heat capacity with and without magnetic fields. For the purpose of good thermal conductivity, the powder sample was pressed into a pellet of 0.5 mm in thickness and 1 mm in diameter. The background of sapphire addenda and N grease was carefully measured in a separate run to acquire the absolute sample heat capacity.

III. RESULTS AND DISCUSSION

A. Magnetic susceptibility

Figure 1 shows the temperature-dependent dc susceptibility (χ), which was performed with an external field of 100 Oe under ZFC process [Fig. 1(a) shows a close-up view at low temperature]. The susceptibility gradually increases with the decrease of temperature from 300 K, then reaches a local maximum around 40 K, which is the manifestation of short-range antiferromagnetic interactions between Fe^{II} ions and is consistent with the Curie-Weiss behavior observed previously. Nevertheless, a negative Curie-Weiss temperature could be deduced at the high-temperature region.[18] Figure 1(b) shows the χT versus T plot and a downward slope at high temperature was observed, which is also an evidence of antiferromagnetic interaction. As the temperature keeps decreasing, a sharp increase of χ is observed at about 20 K, which could be modeled in an Ising-like interaction as follows:

$$\text{---}Fe^{II}(\Delta)\text{—}Fe^{II}(\Lambda)\text{---}Fe^{II}(\Delta)\text{—}Fe^{II}(\Lambda)\text{---}$$

$$J \quad g_a \quad j \quad g_b \quad J \quad g_a \quad j \quad g_b \quad J$$

where g_a and g_b are the Landé factors of Fe^{II} and J and j refer to two different exchange pathways, indicated by the dashed and solid lines, respectively.

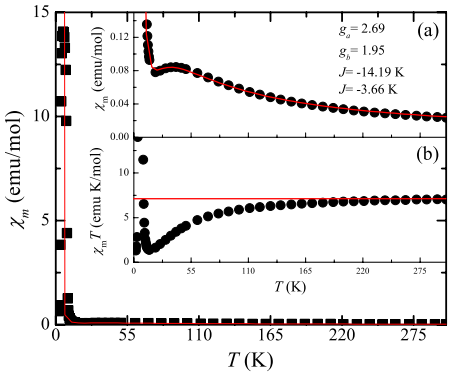

FIG. 1. (Color online) Magnetic susceptibility χ shows a maximum at about 40 K and a divergence at lower temperature, indicating the ferrimagnetic short-range interactions. The red (solid) line is the best fit to the model described in the text. (a) displays the χ on an enlarged scale, (b) displays the χT versus T plot.

For a detailed analysis, we summarized several examples[19–25] in Table I that were treated as the 1D Ising chain, including two different magnetic centers.

Depending on the differentiable exchange coupling, Landé factors, and spin anisotropy among and/or of magnetic centers, the compounds in Table I can be classified as (i) regular antiferromagnetic chains with two different Landé factors ($J=j$; $g_a \neq g_b$),[20,21] and (ii) nonregular antiferromagnetic chains with two different Landé factors ($J \neq j$; $g_a \neq g_b$).[19] Class (iii) is somehow similar to class (i), but also including the anisotropy of the Landé factors ($J=j$; $g_a \neq g_b$; $g_{a\perp} \neq g_{a\parallel}$).[22,23,25] Class (iv) is a modification of class (ii), including the anisotropy of the Landé factors ($J \neq j$; $g_a \neq g_b$; $g_{a\perp} \neq g_{a\parallel}$).[24] The most general case is class (iv), $ReCl_4(\mu\text{-ox})Cu(bipy)_2$, which was handled with a nonregular antiferromagnetic Ising chain model including varied and anisotropic Landé factors.[24] All these compounds have negative J and j values and alternate Landé factors, leading to a ferrimagnetic property at low temperature.

From the characteristics mentioned above, the different bond lengths between Fe^{II} ions (5.515 and 5.523 Å) suggest that J and j are different (i.e., nonregular antiferromagnetic chain). In addition, the recognition of Fe^{II} ions from geometry positions suggests that the Landé factors could be different between $Fe^{II}(\Delta)$ and $Fe^{II}(\Lambda)$. Thereby, we assume that $[Fe^{II}(\Delta)Fe^{II}(\Lambda)(ox)_2(Phen)_2]_n$ is a nonregular antiferromagnetic chain with two different Landé factors, which is quite similar to class (ii). A proper model was suggested by Coronado *et al.* in 1988 in the case of $S=1/2$.[19] The derived temperature-dependent susceptibility can be written as

$$\chi(T) = (N\mu_B^2/2kT)[g_+^2 \exp(J_+/2kT) + g_-^2 \exp(J_-/2kT)]/\cosh(J_-/2kT),$$

with $g_\pm=(g_a \pm g_b)/2$ and $J_\pm=(J \pm j)/2$. For $g_a=g_b$, $\chi(T)$ is reduced to a nonregular antiferromagnetic chain, where χ shows a local maximum at T_{max} and then decreases with decreasing temperature. For $g_a \neq g_b$, a ferrimagnetic behavior occurs (i.e., χ diverges at low temperature) at temperatures

TABLE I. Several example compounds explained by different Landé factors.

Compound	g_a	g_b	J (K)	j (K)	S	Ref.
$Co_2(EDTA)\cdot 6H_2O$	5.33	2.48	−17.5	−0.05	1/2	19
$[Co_2(ox)tpmc](ClO_4)\cdot 3H_2O$	3.42	4.02	−12.9		1/2	20
$Ni_2(EDTA)(H_2O)_4$, $2H_2O$	2.21	2.09	−8.25		1	21
$[Cu(tren)]ReCl_6$	$g_{\parallel Cu}=2.33$ $g_{\perp Cu}=2.01$	$g_{\parallel Re}=1.73$ $g_{\perp Re}=1.72$	−4.46		$S_{Cu}=1/2$ $S_{Re}=3/2$	22
$[CuL]ReBr_6$	$g_{\parallel Cu}=2.29$ $g_{\perp Cu}=1.99$	$g_{\parallel Re}=1.84$ $g_{\perp Re}=1.82$	−5.85		$S_{Cu}=1/2$ $S_{Re}=3/2$	23
$ReCl_4(\mu-ox)Cu(bipy)_2$	$g_{\parallel Cu}=2.33$ $g_{\perp Cu}=2.01$	$g_{\parallel Re}=1.86$ $g_{\perp Re}=1.82$	−11.95	−6.19	$S_{Cu}=1/2$ $S_{Re}=3/2$	24
$[Ni(tetren)]ReCl_6$	$g_{Ni}=2.109$	$g_{Re,z}=1.42$ $g_{Re,x}=1.47$ $g_{Re,x}=1.46$	−3.38		$S_{Re}=3/2$ $S_{Ni}=1$ $S_{Ni}=1$	25
$Fe^{II}(\Delta)Fe^{II}(\Lambda)(ox)_2(Phen)_2$	2.69	1.95	−14.19	−3.66	2	This work

lower than T_{max}. Since Coronado *et al.* established the equation with $S=1/2$, it seems necessary to derive a new equation for our $S=2$ condition. However, the other cases, e.g., $S=1$ and $S=3/2$, were accomplished and behaved quite similar to those of Coronado *et al.*[21–25] Considering the large spin approximation, we have used the same equation with a careful correction owing to the different spin value. The best fit is shown with a solid line in Fig. 1, where $g_a=2.69$, $g_b=1.95$, $J=-14.19$ K, and $j=-3.66$ K, which demonstrates that $[Fe^{II}(\Delta)Fe^{II}(\Lambda)(ox)_2(Phen)_2]_n$ can be described with the 1D ferrimagnetic chain having two different Landé factors. It is noteworthy that we only fit the data at $T>14$ K to avoid the interchain interactions, which construct long-range ordering at lower temperatures and produce a sudden decrease of χ around 8 K. A similar fitting process has been used for other systems.[26] The long-range ordered ground state was confirmed by neutron diffraction and the observation of a λ-type anomaly of specific heat, which will be discussed as follows.

B. Neutron diffraction

Complete structural analysis of the sample was made by employing neutron powder diffraction, and the pattern was analyzed by using the General Structure Analysis System (GSAS) program,[27] following the Rietveld refinement method. Figure 2 shows the observed (crosses) and the fitted (solid lines) patterns of the compound taken at room temperature, with their differences plotted at the bottom. This pattern can be described well using monoclinic symmetry with the space group $P2_1$, which is consistent with the reported results that use x-ray diffraction.[18] The refined structural parameters are listed in Table II. No traces of impurity phases were found. We estimate the impurity phase in the sample to be less than 2%. The chainlike compound $[Fe^{II}(\Delta)Fe^{II}(\Lambda)(ox)_2(Phen)_2]_n$ consists of bimetallic oxalate groups as a backbone bridging with incorporated phen groups, which may cause long-range interactions by constructing π-stacked structures between adjacent chains.[28] The results of refinement show that the local environments of two Fe^{II}, such as bond length and angle, are different. Moreover, the period of crystal framework in $[Fe^{II}(\Delta)Fe^{II}(\Lambda)(ox)_2(Phen)_2]_n$ is geometrically constructed by cooperating with phen groups between interchains. The π-π interaction between phen groups offers numerous opportunities for studying the geometrically frustrated magnetic system and the problem of dimensionality due to its weak, instead of strong, bonding in the solid crystal. The intrachain interaction of magnetic centers in low dimensional structures generally induces the short-range correlation before the construction of LRMO as the temperature decreases.

The basic spin configuration can be determined from the angular positions of the magnetic diffraction pattern. The

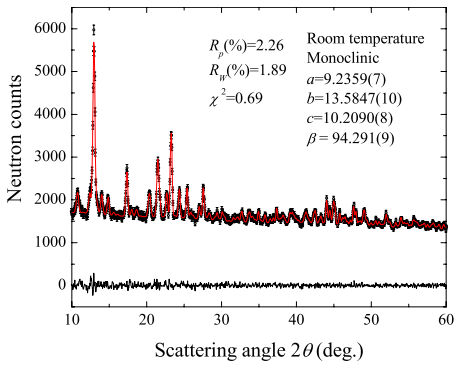

FIG. 2. (Color online) Crystal refinement by neutron diffraction at room temperature, where the data (cross) and fitted line (red) are represented. Detailed structural parameters are listed in Table II.

TABLE II. Refined structural parameters of $[Fe^{II}(\Delta)Fe^{II}(\Lambda)(ox)_2(Phen)_2]_n$ calculated from neutron diffraction patterns taken at room temperature.

Structure: Monoclinic
Space group: $P2_1$
$R_p(\%)=2.26$, $R_W(\%)=1.89$, $\chi=0.69$
$a=9.2359(7)$ Å, $b=13.5847(10)$ Å, $c=10.2090(8)$ Å
$\alpha=\gamma=90$, $\beta=94.291(9)$

Atom	x	y	z
Fe1	0.115(7)	0.9587(40)	0.394(6)
Fe2	0.614(4)	0.9790(31)	0.109(4)

Bond length (Å)		Bond angle (deg)	
Fe(1)–O(2)	2.12(10)	O(2)–Fe(1)–O(8)	88.(6)
Fe(1)–O(6)	2.18(8)	O(2)–Fe(1)–N(1)	106.(4)
Fe(1)–O(8)	1.96(18)	O(8)–Fe(1)–N(1)	121.(6)
Fe(1)–O(1)	2.40(8)	O(3)–Fe(2)–O(5)	95.(5)
Fe(1)–N(1)	2.39(8)	O(3)–Fe(2)–O(7)	102.(4)
Fe(1)–N(2)	2.11(7)	O(5)–Fe(2)–O(7)	79.(5)
Fe(2)–O(4)	2.16(12)	O(3)–Fe(2)–N(4)	95.6(28)
Fe(2)–O(5)	1.97(12)	O(5)–Fe(2)–N(4)	87.(4)
Fe(2)–O(7)	2.01(11)	O(7)–Fe(2)–N(4)	158.(4)
Fe(2)–O(3)	2.15(9)		
Fe(2)–N(3)	2.18(6)		
Fe(2)–N(4)	2.10(6)		

magnetic diffraction pattern that we obtained at 1.4 K is shown in Fig. 3, where the diffraction pattern taken at 18 K, serving as the nonmagnetic background, has been subtracted from the 1.4 K data. The pattern of their differences reveals Bragg peaks that developed as the temperature was reduced from 18 to 1.4 K, signifying the Fe^{II} spin ordering. The widths of these magnetic peaks are resolution limited, indicating a three-dimensional long-range magnetic ordering for the Fe^{II} spins. The indices marked on the magnetic peaks are

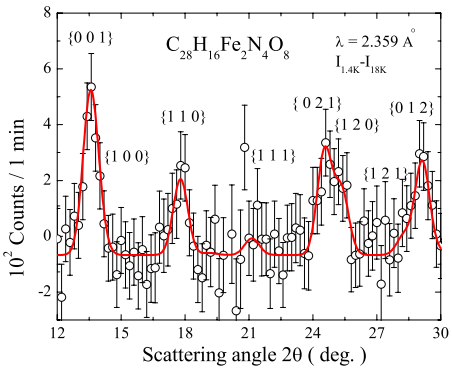

FIG. 3. (Color online) Neutron scattering counts obtained by $I_{1.4\ K}-I_{18\ K}$, which shows the diffraction due to the magnetic ordering. The red line shows the calculated pattern based on the spin model shown in Fig. 4.

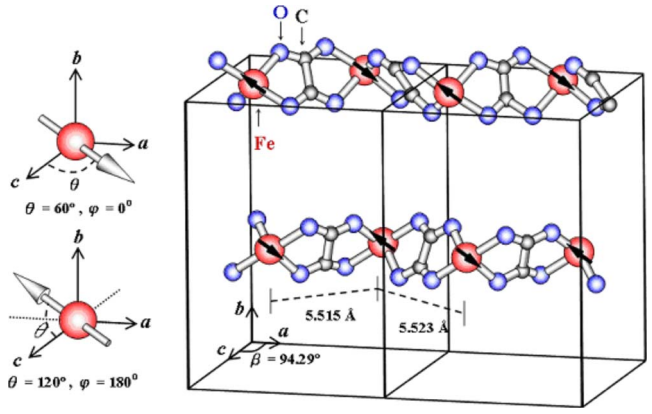

FIG. 4. (Color online) Antiferromagnetic spin structure obtained from the magnetic Bragg pattern.

based on the nuclear unit cell. Only whole integers are needed for indexing the magnetic peaks, showing that the magnetic unit cell is the same as the nuclear one. This, however, does not necessarily indicate a ferromagnetic structure for the Fe^{II} ions, since there are two Fe^{II} ions both along a and b crystallographic directions in one unit cell, implying an antiparallel spin arrangement that can be sufficiently described as the nuclear one. On the contrary, the magnetic moment must be arranged ferromagnetically along the c crystallographic direction, since there is only one Fe^{II} ion in the unit cell along this direction. The magnetic structure that fits the observed magnetic diffraction pattern is shown in Fig. 4. The spin configuration found for the Fe^{II} ions consists of simple antiparallel arrangements of Fe^{II} spins both along a and b crystallographic directions and parallel to the c crystallographic direction, with the moment lying in the ac plane and slightly off the phen center. It is clear that there are two simple antiferromagnetic chains along the a crystallographic direction. In Fig. 3, the solid line shows the calculated pattern, based on the spin model shown in Fig. 4, indicating that the proposed model fits nicely to the observed pattern. This proposed magnetic structure was obtained on a powder sample and by using the data of large statistical fluctuations, and therefore, might require further investigation. The thermal average of the z component of the magnetic moment $\langle\mu_Z\rangle$ per formula unit at 1.4 K,[29] obtained by comparing the low-temperature magnetic intensities to the nuclear ones, is $\langle\mu_Z\rangle=0.42(6)\mu_B$. It also confirms the magnitude of saturation magnetization ~3.5 emu/g or $0.41\mu_B$ formula unit at 2.5 K, as was observed in the previous study.[18] The difference between the effective moment ($5.59\mu_B$, $T>T_m$, from Curie-Weiss fit) and ordered moment ($0.42\mu_B$, $T<T_m$, from neutron magnetic scattering) arises from the difference between the average free moments above T_m without any interaction and average moments below T_m with interactions that partially cancel each other out.

If the peaks evolved in a different pattern have a magnetic origin, then their intensities must vary with temperature, and thereby, should give an idea about the transition temperature. Figure 5 shows the temperature dependence of the {001} peak intensity. At low temperatures, it reveals a typical order parameter measurement for a powder sample, showing the

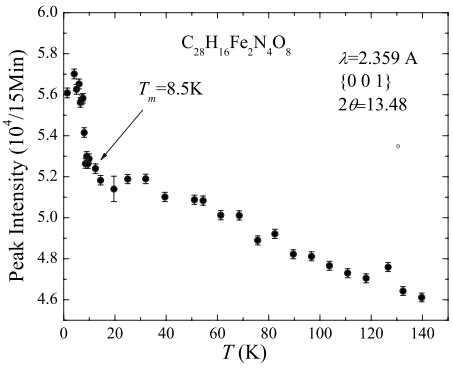

FIG. 5. Temperature dependence of peak intensity of {001} shows the onset of the LRMO at 8.6 K, and that the short-range correlation starts from high temperature.

ordering temperature, as determined by the inflection point, of $T_m \sim 8.6$ K for the Fe^{II} ions. In addition, a noticeable increase in the {001} intensity is also found while the temperature decreases from 140 K. The amount of increase in the {001} intensity in the high-temperature regime is comparable to those developed at low temperatures, originated from the Fe spin ordering. Note that these data were taken with a PG (002) analyzer crystal which was placed in front of the detector to discriminate against background and inelastic scattering. The substantial amount of increase in the {001} intensity cannot originate solely from the increase in the background scattering. These data signify the development of short-range correlations below 140 K.

C. Specific heat

Low-temperature specific heat measurements of $[Fe^{II}(\Delta)Fe^{II}(\Lambda)(ox)_2(Phen)_2]_n$ were performed within the temperature range 0.6–20 K, both with and without magnetic field. C/T as a function of temperature was plotted in Fig. 6. There is an obvious anomaly around 8 K, which could be related to the ordering of the spin degree of freedom. In addition, the background, showing a monotonic increase with temperature, is due to the lattice contribution, which is typically described by the Debye model. The zero-field data, by removing the robust peak points, could be fitted well to the integrated Debye model

$$C_v = 9Nk_B\left(\frac{T}{\Theta_D}\right)^3 \int_0^{\Theta_D/T} \frac{x^4 e^x}{(e^x-1)^2} dx.$$

The nonmagnetic background is not significantly affected by the external field [see Fig. 7(a)]; here, it is only related to the lattice contribution because of the insulating behavior in the molecular magnet. The derived Debye temperature Θ_D as a fitting parameter comes out to be 73 K. Such a low-dimensional structure usually leads to saturation of heat capacity at relatively low temperatures due to the weak bonding interactions between the interchain molecules. The small Θ_D was also observed in previously reported SMM because of the low-dimensional structure (see Table III, Refs. 26 and 30–42.

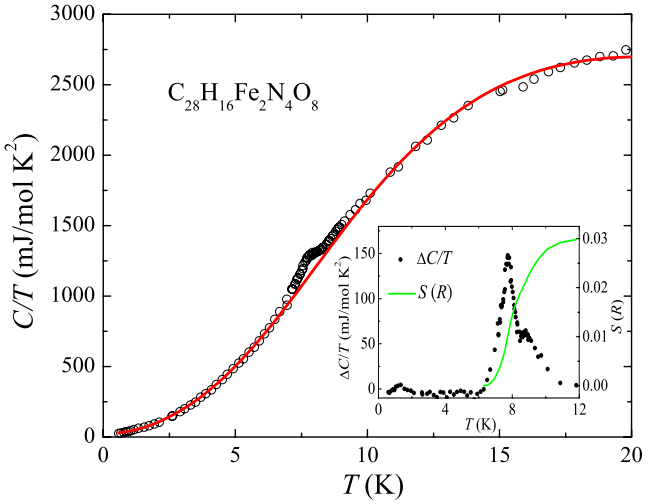

FIG. 6. (Color online) Upper panel is plotted as C/T vs T for $[Fe^{II}(\Delta)Fe^{II}(\Delta)(ox)_2(Phen)_2]_n$ at zero field. The red line is the lattice contribution by fitting to the Debye model. The inset shows the magnetic anomaly and the estimated entropy.

In the inset of Fig. 6, we show the remnant magnetic ordering which is obtained by subtracting the nonmagnetic background. The magnitude of the jump, namely, $\Delta C/T_m$, corresponding to the interaction between the magnetic clusters, is found to be only 0.15 J/mol K^2. The magnetic entropy could be derived from integrating the area of the phase transition peak, $S/R = \int_0^T (C_m/T)dT$, where R is the universal

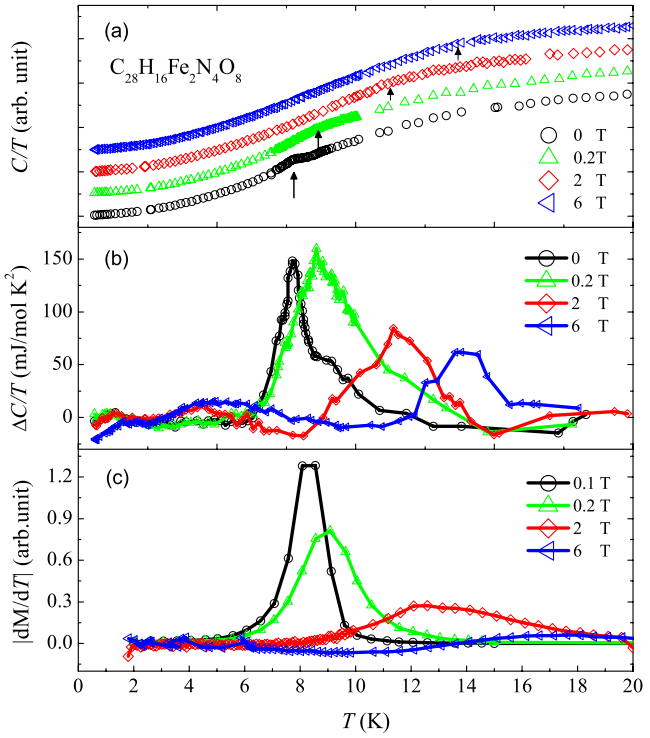

FIG. 7. (Color online) Temperature and magnetic field dependences of (a) specific heat (offset for clarity), (b) specific heat anomaly, and (c) temperature derivative of magnetization.

TABLE III. Comparative results of various molecular magnet compounds. The following notations are defined as T_C, ferromagnetic transition temperature; T_N, antiferromagnetic ordering temperature; T_B, blocking temperature; Θ_D, Debye temperature; and S, effective spin value, with LRMO indicating long-range magnetic ordering.

Compound	T_C (K)	T_N (K)	T_B (K)	Θ_D (K)	S	LRMO	Ref.
$CuMn(S_2C_2O_2)_2(H_2O)_3\cdot 4.5H_2O$						Y	26
Mn_4Cl				15	9/2	N[a]	30
Mn_4Br		1.33		108	9	Y	31
Mn_6	0.15			48	12	Y	32
$Mn_{12}Ac$	0.90		3.0	38	10	Y[b]	33–35
$Mn_{12}Pr$			3.5	30	9	N	36
Fe_{12}				150	5/2		37
Fe_{17}	0.81			23	35/2	Y	38
Fe_{19}		1.19			33/2	Y	39
Fe_{14}		1.87		10	25	Y	40
$Mn[N(CN)_2]_2(pyz)$		2.53			5/2	Y	41
$MnCu(opba)(H_2O)_2\cdot DMSO$		5				Y	42
$C_{28}H_{16}Fe_2N_4O_8$		8.6		73	4	Y	This work

[a]Mn_4Cl has a λ-type anomaly at 7 K, which is of nonmagnetic origin, probably associated with a structural transition.

[b]The LRMO of $Mn_{12}Ac$ is not revealed in specific heat measurement, but is confirmed by neutron diffraction.

gas constant, giving a relatively small value, $S=0.03R$. The theoretical magnitude of the magnetic entropy difference between spin ordering and disordering states can be simplified as $S=R\ln(2S+1)$. In the ideal case, Fe^{II} ($S=2$) gives the magnetic entropy $S=1.6R$. The experimental value only contributes 1.9% of the theoretical one. This may be due to the fact that above T_m, there still exist some ordering (short range) of the spins and, as a result, a minimum fluctuation occurs even at $T>T_m$. Below T_m, it changes into long-range magnetic ordering. The negligible amount of entropy was frequently observed in the low-dimensional spin system; for example, a quasi-one-dimensional antiferromagnet $(CH_3)_4NMnCl_3$, whose residual entropy below the Néel temperature was estimated to be 1% of total magnetic entropy.[43]

The LRMO below T_m could arise from the increase of interchain π-π interaction with decreasing temperature. Therefore, the crystalline structure builds a much stronger 3D lattice framework instead of loosely independent chains, and consequently, reduces the difference of Landé factors. As mentioned above, the different Landé factors of two Fe^{II} ions cause a net moment and form a ferrimagnetic state. The decrease of the difference of Landé factors will reduce the net moments, which could account for the sudden drop of the χ vs T curve below 8 K.

In Fig. 7, there are two interesting phenomena under the effect of an external magnetic field which may have different origins. First, the magnetic-field-dependent specific heat plotted in C/T vs T shows that the small robust λ-type anomaly is shifted to higher temperature due to the application of a magnetic field. It is consistent with the field-dependent magnetization and reveals that the magnetic field promotes the formation of LRMO. A traditional antiferromagnetic material shows that the λ-type anomaly is shifted toward lower temperature by an applied magnetic field.[44] However, the behavior of the present compound is different from that. It may be due to the fact that the studied system is ferrimagnetic. Secondly, there is a small anomaly located around 1 K under the low field, which gradually becomes a hump at around 5 K under a magnetic field of 6 T, but is not clearly seen from corresponding magnetization data. From the results of an earlier report,[34] the energy level splitting caused by the internal crystal field can be seen from specific heat and conforms to a model where the double wells are separated by the energy barrier. By applying an external magnetic field, the symmetry and degeneracy of m_s (spin quantum number) states are broken, leading to an extra field-dependent Schottky anomaly of the Zeeman splitting states.[45] Each of the spin states could be thermally lifted to an excited state with an increasing field, but the distributed spins among energy levels pass through the energy barrier with different probabilities. This scenario would, in fact, describe the results of our field-dependent data, where the small anomaly is

broadened and shifted to higher temperature. Definitely, more experiments and quantitative analyses are needed to further confirm this scenario.

As low-dimensional systems are not prone to construct long-range ordering, it is difficult to verify such a long-range magnetic ordering in such system. We collected some examples in Table III in order to compare different instances of LRMO. The first way to prove LRMO is to find the λ-type anomaly in the specific heat measurement, as in our work and for many other SMM.[30–41] However, for the ideal SMM, the spin-lattice relaxation becomes very slow below the blocking temperature because of the large anisotropy barrier and lack of phonon, and the fact that the thermal equilibrium requires too much time. Consequently, it is difficult to measure specific heat at such a low temperature, even if there exist some LRMO. The second way is to measure the variation in the magnetic peaks with temperature by performing a neutron diffraction experiment. The typical example is $Mn_{12}AC$, in which long-range magnetic ordering is not confirmed by specific heat but by neutron diffraction.[46] The third way is to analyze magnetic susceptibility behavior by employing the existing model.[22,25,26,42] In our work, all three techniques are used, which gave consistent results to confirm that $[Fe^{II}(\Delta)Fe^{II}(\Lambda)(ox)_2(Phen)_2]_n$ exhibits LRMO at $T<8.6$ K. In addition, in Table III, we can clearly see that the SMM usually shows LRMO at temperatures lower than that of chainlike compounds. It may be due to the lack of interaction between SMM particles. Furthermore, among the chainlike compounds, $[Fe^{II}(\Delta)Fe^{II}(\Lambda)(ox)_2(Phen)_2]_n$ exhibits LRMO at a much higher temperature, suggesting that the interaction between chains of $[Fe^{II}(\Delta)Fe^{II}(\Lambda)(ox)_2(Phen)_2]_n$ is relatively strong. The T_c is believed to be strongly influenced by the dimensionality of the molecular-base magnet, for example, a layered molecular magnet (2D) which also uses Fe^{II} ions as magnetic center shows ferrimagnetic ordering around 90 K,[47] and the well-known Prussian bluelike structure complexes, which are created in a 3D framework, give a higher T_c at around room temperature.[48–50]

IV. CONCLUSION

$[Fe^{II}(\Delta)Fe^{II}(\Lambda)(ox)_2(Phen)_2]_n$ has been studied by magnetization, neutron diffraction, and field-dependent specific heat measurement to clarify the nature of its magnetic properties. There are several prominent findings: (1) At the high-temperature region ($T>T_m$), the short-range fluctuated spin ordering follows an Ising chain model with two different Landé factors, which leads to a ferrimagnetic behavior. (2) At the low-temperature region ($T<T_m$), the long-range antiparallel alignment between the spins of Fe^{II} ions is derived by neutron diffraction and specific heat measurements. However, the different g values of Fe^{II} ions leads to a net ferrimagnetic structure. (3) The entropy, estimated from the specific heat anomaly, is only about 1.9% of the expected theoretical value, indicating the low-dimensional character of magnetic ordering at $T<T_m$ and the short-range spin fluctuations in high temperatures. (4) Application of a magnetic field shifts the value of T_m toward the higher temperature regime, indicating that the magnetic field promotes the formation of LRMO.

ACKNOWLEDGMENTS

We are grateful to W. N. Mei for his stimulating discussion. This work was supported by the National Science Council of Taiwan under Contracts Nos. NSC 95-2112-M-110-023 and NSC 94-2113-M-005-004.

*Corresponding author; yang@mail.phys.nsysu.edu.tw

[1] M. N. Leuenberger and D. Loss, Nature (London) **410**, 789 (2001).
[2] S. M. J. Aubin, N. R. Dilley, L. Pardi, J. Krzystek, M. W. Wemple, L. C. Brunel, M. B. Maple, G. Christou, and D. N. Hendrickson, J. Am. Chem. Soc. **120**, 4991 (1998).
[3] K. Wieghardt, K. Pohl, I. Jibril, and G. Huttner, Angew. Chem., Int. Ed. Engl. **23**, 77 (1984).
[4] A. L. Barra, A. Caneschi, A. Cornia, F. F. de Biani, D. Gatteschi, C. Sangregorio, R. Sessoli, and L. Sorace, J. Am. Chem. Soc. **121**, 5302 (1999).
[5] S. L. Castro, Z. M. Sun, C. M. Grant, J. C. Bollinger, D. N. Hendrickson, and G. Christou, J. Am. Chem. Soc. **120**, 2365 (1998).
[6] T. Mallah, C. Auberger, M. Verdaguer, and P. Veillet, J. Chem. Soc., Chem. Commun. **1995**, 61.
[7] A. Scuiller, T. Mallah, M. Verdaguer, A. Nivorozkhin, J. L. Tholence, and P. Veillet, New J. Chem. **20**, 1 (1996).
[8] A. Scuiller, V. Marvaud, J. Vaissermann, I. Rosenman, and M. Verdaguer, Mol. Cryst. Liq. Cryst. Sci. Technol., Sect. A **334**, 1165 (1999).
[9] Y. C. Zhong, M. P. Sarachik, J. Yoo, and D. N. Hendrickson, Phys. Rev. B **62**, R9256 (2000).
[10] T. Lis, Acta Crystallogr., Sect. B: Struct. Crystallogr. Cryst. Chem. **36**, 2042 (1980).
[11] A. Caneschi, D. Gatteschi, R. Sessoli, A. L. Barra, L. C. Brunel, and M. Guillot, J. Am. Chem. Soc. **113**, 5873 (1991).
[12] R. Sessoli, H.-L. Tsai, A. R. Schake, S. Wang, J. B. Vincent, K. Folting, D. Gatteschi, G. Christou, and D. N. Hendrickson, J. Am. Chem. Soc. **115**, 1804 (1993).
[13] M. A. Novak, R. Sessoli, A. Caneschi, and D. Gatteschi, J. Magn. Magn. Mater. **146**, 211 (1995).
[14] L. Gunther and B. Barbara, *Quantum Tunneling of Magnetization-QTM '94* (Kluwer Academic, Boston, 1995).
[15] A. Caneschi, D. Gatteschi, N. Lalioti, C. Sangregorio, R. Sessoli, G. Venturi, A. Vindigni, A. Rettori, M. G. Pini, and M. A. Novak, Angew. Chem., Int. Ed. **40**, 1760 (2001).
[16] N. E. Chakov, W. Wernsdorfer, K. A. Abboud, and G. Christou, Inorg. Chem. **43**, 5919 (2004).
[17] C. Coulon, H. Miyasaka, and R. Clérac, Struct. Bonding (Berlin) **122**, 163 (2006).
[18] L. L. Li, K. J. Lin, C. J. Ho, C. P. Sun, and H. D. Yang, Chem.

Commun. (Cambridge) **12**, 1286 (2006).
[19] E. Coronado, M. Drillon, P. R. Nugteren, L. J. de Jongh, and D. Beltran, J. Am. Chem. Soc. **110**, 3907 (1988).
[20] N. Dj. Lazarov, V. Spasojevic, V. Kusigerski, V. M. Matic, and M. Milic, J. Magn. Magn. Mater. **272**, 1065 (2003).
[21] E. Coronado, M. Drillon, A. Fuertes, D. Beltran, A. Mosset, and J. Galy, J. Am. Chem. Soc. **108**, 900 (1986).
[22] A. Tomkiewica, A. Zygmunt, and J. Mrozinski, J. Mol. Struct. **644**, 97 (2003).
[23] A. Tomkiewicz, B. Korybut-Daszkiewcz, A. Zygmunt, and J. Mrozinski, J. Mol. Struct. **613**, 115 (2002).
[24] R. Chiozzone, R. González, C. Kremer, G. De Munno, J. Cano, F. Lloret, M. Julve, and J. Faus, Inorg. Chem. **38**, 4745 (1999).
[25] A. Tomkiewicz, R. Boca, M. Nahorska, and J. Mrozinski, J. Mol. Struct. **734**, 143 (2005).
[26] A. Gleizes and M. Verdaguer, J. Am. Chem. Soc. **106**, 3727 (1984).
[27] A. C. Larson and R. B. Von Dreele, Los Alamos National Laboratory Report No. LA-UR-86-748, 2000 (unpublished).
[28] E.-Q. Gao, S.-Q. Bai, Z.-M. Wang, and C.-H. Yan, J. Am. Chem. Soc. **125**, 4984 (2003).
[29] J. W. Lynn, J. A. Gotaas, R. N. Shelton, H. E. Horng, and C. J. Glinka, Phys. Rev. B **31**, 5756 (1985).
[30] M. Evangelisti, F. Luis, F. L. Mettes, N. Aliaga, G. Aromí, J. J. Alonso, G. Christou, and L. J. de Jongh, Phys. Rev. Lett. **93**, 117202 (2004).
[31] A. Yamaguchi, N. Kusumi, H. Isimoto, H. Mitamura, T. Goto, N. Mori, M. Nakano, K. Awaga, J. Yoo, D. N. Hendrickson, and G. Christou, J. Phys. Soc. Jpn. **71**, 414 (2002).
[32] A. Morello, F. L. Mettes, F. Luis, J. F. Fernández, J. Krzystek, G. Aromí, G. Christou, and L. J. de Jongh, Phys. Rev. Lett. **90**, 017206 (2003).
[33] F. L. Mettes, F. Luis, and L. J. de Jongh, Phys. Rev. B **64**, 174411 (2001).
[34] A. M. Gomes, M. A. Novak, R. Sessoli, A. Caneschi, and D. Gatteschi, Phys. Rev. B **57**, 5021 (1998).
[35] M. Evangelisti, F. Luis, L. J. de Jongh, and M. Affronte, J. Mater. Chem. **16**, 2534 (2006).
[36] Y. Miyazaki, A. Bhattacharjee, M. Nakano, K. Saito, S. M. J. Aubin, H. J. Eppley, G. Christou, D. N. Hendrickson, and M. Sorai, Inorg. Chem. **40**, 6632 (2001).
[37] M. Affronte, J. C. Lasjaunias, and G. L. Abbati, Phys. Rev. B **66**, 180405(R) (2002).
[38] M. Evangelisti, A. Candini, A. Ghirri, M. Affronte, G. W. Powell, I. A. Gass, P. A. Wood, S. Parsons, E. K. Brechin, D. Collison, and S. L. Heath, Phys. Rev. Lett. **97**, 167202 (2006).
[39] M. Affronte, J. C. Lasjaunias, W. Wernsdorfer, R. Sessoli, D. Gatteschi, S. L. Heath, A. Fort, and A. Rettori, Phys. Rev. B **66**, 064408 (2002).
[40] M. Evangelisti, A. Candini, A. Ghirri, M. Affronte, E. K. Brechin, and E. J. L. McInnes, Appl. Phys. Lett. **87**, 072504 (2005).
[41] A. L. Manson, Q.-Z. Huang, J. W. Lynn, H.-J. Koo, M.-H. Whangbo, R. Bateman, T. Otsuka, N. Wada, D. N. Argyriou, and J. S. Miller, J. Am. Chem. Soc. **123**, 162 (2001).
[42] H. O. Stumpf, Y. Pei, L. Ouabab, F. Le Berre, E. Codjovi, and O. Kahn, Inorg. Chem. **32**, 5687 (1993).
[43] F. Borsa, M. G. Pini, A. Rettori, and V. Tognetti, Phys. Rev. B **28**, 5173 (1983).
[44] Allan H. Morrish, *The Physical Principles of Magnetism* (Wiley, New York, 1965), Chap. 8, p. 457.
[45] M. Sorai, M. Nakano, and Y. Miyazaki, Chem. Rev. (Washington, D.C.) **106**, 976 (2006).
[46] F. Luis, J. Campo, J. Gomez, G. J. McIntyre, J. Luzon, and D. Ruiz-Molina, Phys. Rev. Lett. **95**, 227202 (2005).
[47] K. I. Pokhodnya, M. Bonner, J.-H. Her, P. W. Stephens, and J. S. Miller, J. Am. Chem. Soc. **128**, 15592 (2006).
[48] V. Gadet, T. Mallah, I. Castro, and M. Verdaguer, J. Am. Chem. Soc. **114**, 9213 (1992).
[49] K. J. Nelson, I. D. Giles, S. A. Troff, A. M. Arif, and J. S. Miller, Inorg. Chem. **45**, 8922 (2006).
[50] K. S. Min, A. DiPasquale, A. L. Rheingold, and J. S. Miller, Inorg. Chem. **46**, 1048 (2007).